

ARTICLES

C-14 AGE PROFILES FOR ANCIENT SEDIMENTS AND PEAT BOGS

R. H. Brown

Director, Geoscience Research Institute

It is sometimes proosed that the correlation between C-14 ages and depth as found in peat bogs and sediments demonstrates the validity of the C-14 dating technique. The comprehensive study presented below shows that such a conclusion is not warranted, since, in the great majority of cases, a linear relationship between depth and C-14 concentration does not exist.

INTRODUCTION

In the development of the radiocarbon dating technique, it was recognized that calibration against an independent method of dating past events was necessary for conversion of radioactive carbon measurements into real time. After the development of this technique Dr. Willard Libby was able to demonstrate an approximate one-to-one correspondence between radiocarbon age and real time over a range extending from the present into the early part of the second millennium B.C., provided that the specimen received its carbon from the biosphere during a relatively brief interval of time and was effectively isolated chemically since that time (Libby 1955). Hl. de Vries, H. E. Suess, M. Stuiver and Elizabeth Ralph, utilizing dendrochronological techniques, subsequently led out in the development of refinements for converting C-14 ages into real time (See Olsson 1970). The work of C. W. Ferguson to extend conversion of C-14 dates over an additional three millennia to beyond 7000 B.P. ("before the present") using bristlecone pine wood is well known (Olsson 1970). Excellent conversion charts and graphs covering the range from A.D. 1800 to 5350 B.C. have been published recently by the University of Pennsylvania (Ralph et al. 1973).

There is need for a basis on which to interpret radiocarbon ages in excess of 8000 B.P. other than by uncertain extrapolation. Furthermore, the presently available conversion system covering the 4000 to 8000 B.P. range rests on an insecure foundation due to the unique problems of bristlecone pine dendrochronology (insensitivity of growth ring sequences) and the reliance on C-14 dating to establish a master ring chronology which in turn is used to calibrate C-14 ages. Bristlecone pine dendrochronology presently supports the concept that prior to 1000 B.C. the relative C-14 level in Earth's atmosphere was higher than the value that has been maintained with little variation over the past three millennia.



FIGURE 1. Section through an ancient peat bog near the town of Sydney Mines, Nova Scotia, Canada. The peat is the darker and thicker layered material which forms the main part of the picture; it rests on lighter colored lithified sediments.

The investigation reported in this paper was undertaken in the hope of making some progress toward a better understanding of the relative C-14 activity in the biosphere during prehistoric times and toward an improved perception of the real time significance that may be attached to C-14 ages.

PEAT AND SEDIMENT PROFILE OBSERVATIONS

Peat bogs (Figure 1) and sediments that involve organic material contain information concerning C-14 activity in the biosphere that covers

the entire range of radiocarbon dating to “infinite age.” Unfortunately, this information is available only in a relation between two dependent variables. The three-dimensional relationship between radiocarbon age, feature depth and real time can only be seen in projection on the plane in which a C-14 age versus feature depth profile may be displayed. Real time is a hidden variable that extends normal to this plane. Lacking direct data concerning the relationship between either feature depth or C-14 age and real time, we can hope that a study of the empirical relationships between these two dependent variables will enable us to draw some useful and soundly based conclusions concerning the manner in which either of them have related to real time.

Idealized relationships that may be expected between C-14 age and feature or formation depth are illustrated in Figure 2. In plotting these profiles, I have chosen to present C-14 age on the ordinate axis to emphasize that it is a dependent variable. Plots of C-14 age versus depth can be visually classified as A-type, B-type and C-type. Under strictly uniform conditions an A-type linear profile would be produced. Real-time-dependent changes in the relative C-14 activity of the biosphere or in the rates at which sediments and bogs accumulate could produce profiles of either the B-type (convex toward the depth axis) or the C-type (concave toward the depth axis). Samples of A-, B- and C-type profiles that have been reported in the literature are shown in Figures 3, 4 and 5, respectively.

FIGURE 2. PROFILE TYPE ILLUSTRATION. The departure of the extreme age point from a linear relationship is given by δ . The C-14 age range over which the deeper portion of the profile departs from linearity is given by γ .

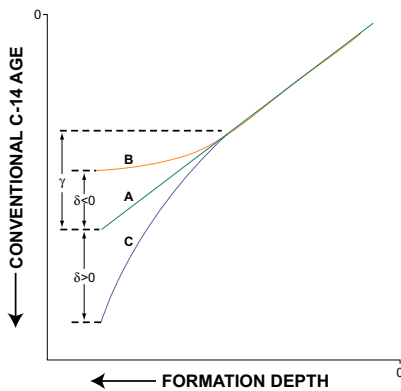
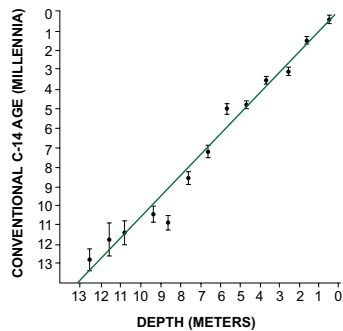


FIGURE 3. SAMPLE A-TYPE PROFILE. Torren's Bog (See Table 1).



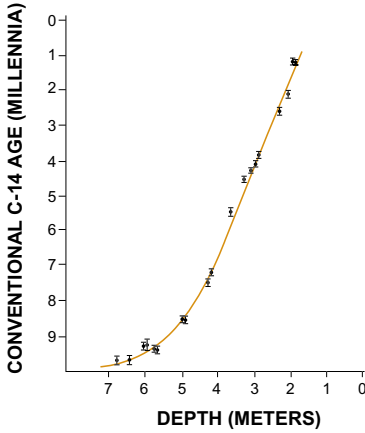


FIGURE 4. SAMPLE B-TYPE PROFILE. Trummen (See Table 1).

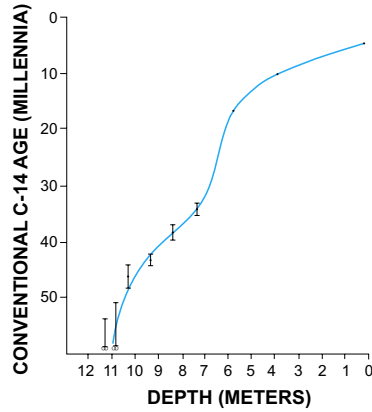


FIGURE 5. SAMPLE C-TYPE PROFILE. Padul IV (See Table 1).

Variants of the C-type are illustrated in Figures 6 and 7. Each point represents the measured value and \pm one standard error.

To make the analysis of a large number of features as objective as possible, a quantitative description of feature profile is necessary. The ordinary mathematical description of curvature would be useful only for profiles that are a straight line or a segment of a circle. A shape factor designation that has been found useful describes the profile in terms of the departure of the extreme end point (maximum age) from a linear relationship. As depicted in Figure 2, we set δ equal to the amount by which the C-14 age for the extreme end point departs from a linear relationship. The C-14 age range over which the extreme age portion of the profile is non-linear is represented by γ . This construction assumes that a straight line can be satisfactorily fitted to the data points for a more recent portion of the feature.

The profile shape factor S may then be defined as a logarithmic function given by Equation 1.

$$S = \ln (1 + \delta/\gamma) \quad \text{Equation 1}$$

Accordingly

- $S = 0$ for strict A-type profiles,
- $-\infty < S < 0$ for the B-type profile range of possibility,
- $0 < S < +\infty$ for the C-type profile range of possibility.

TABLE 1

FEATURE TABULATION

Reference is to **Radiocarbon** (New Haven, CT: Yale University), **volume**:page, unless noted otherwise. C-14 Age Range gives the total range in conventional C-14 years (5570 year half-life) of profile data given in the stated reference. Shape Factor is described in connection with Equation 1 of the accompanying text. Asterisk (*) indicates non-linear profile shape based on only one datum point at maximum of age range.

FEATURE	REFERENCE	C-14 AGE RANGE	PROFILE SHAPE FACTOR
A-Type Profile			
PEAT			
Hangklip, S. Africa	12:453	360 - 11,140	0
Red Moss Bog, England	12:592	4,370 - 9,798	0
Ballynagilly, Ireland	13:112	695 - 9,595	0.23
Tregaron S. E. Bog, Wales	14:240	2,922 - 10,205	0
Stockbergsmymren, Sweden	9:392	430 - 9,280	0
Sur-Les-Bieds, France	9:031	4,430 - 9,360	0.14
Kirchner Marsh, Minnesota	5:312	1,660 - 10,230	0 - 0.17 [0.08]
Torren's Bog, Ohio	9:324	420 - 10,960	0
Hershop Bog, Texas	12:253	1,520 - 10,920	0
SEDIMENT			
Sacred Lake #3, Kenya	12:448	3,285 - 33,350	0
Zombepata Cave, Rhodesia (charcoal)	15:550	2,110 - 37,290	0
Lake Victoria, Uganda (Pilkington Bay)	11:600	3,240 - 14,730	0 - 0.25 [0.12]
Kyoto, Japan	15:042	7,050 - 12,340	0
Lake Zeribar, Iran	11:593	8,100 - 22,000	0
Belle Lake, Ireland	16:007	5,490 - 12,235	0
Lake Vuolep Njakojaure, Sweden (shallow)	11:442	2,370 - 9,420	0
Selent Lake V, Germany	15:276	106 - 14,180	0?
Round Lake, Indiana	15:361	655 - 9,345	0
Myrtle Lake, Minnesota	11:575	2,680 - 11,120	0
Mediterranean Core 95	15:390	2,835 - 13,895	0
Middle American Trench, W. Coast of Mexico	10:270	2,080 - 11,500	0
Walvis Ridge, S. Atlantic	11:651	4,320 - 37,000	0
B-Type Profile			
PEAT			
Hallarums Mosse, Sweden	9:404	4,585 - 10,170	-0.82
S. Mjölstötmyren (B), Sweden	9:389	765 - 9,725	-0.72
Råbacka, Finland	10:269	3,510 - 9,430	-1.05
Jewell Bog, Iowa	10:255	2,365 - 11,640	-1.43
Denmark Bog, New Jersey	9:323	2,290 - 11,500	-0.53
Boriack, Texas	12:625	3,700 - 15,460	-0.35
Valle de Laguinillas, Colombia	11:355	6,510 - 12,320	-2.12
SEDIMENT			
Gandiol, Senegal	16:080	2,000 - 34,300	-2.37*
Lake Nojiri, Japan	11:595	1,530 - 11,800	-0.42

TABLE 1 (continued)

Timor Sea, Indonesia	9:279	2,320 - 19,000 and >30,000	-2.16*
Trummen, Sweden	10:040; 11:434; 12:535	1,130 - 11,730	-0.50
Selent Lake #IIN.W. Germany	15:273	1,300 - 24,830	-1.11 - 0 [-0.55]
Mid-Atlantic Ridge, S. Atlantic	11:651	5,940 - 30,100	-0.92
C-Type Profile			
PEAT			
Altnahinch, Ireland	15:220	1,525 - 9,555	0.53
Slieve Gallion, Ireland	13:113	2,670 - 9,660	0.54
Sluggan, Ireland	12:296; 13:124; 454,465; 16:272	985 - 12,360	0.82
Din Moss, Scotland	15:536	5,341 - 12,251	1.10
Ageröd, Sweden	5:208	430 - 10,680	1.43
Barsebäckmossen, Sweden	15:496	4,810 - 9,640	1.74
Hallviken, Sweden	9:395	1,305 - 9,860	0.32
Tisjön, Sweden	5:207	720 - 7,630	0.85
Meldorf, W. Germany	9:224	2,690 - 11,950	1.02
Hanhijänkä, Finland	16:254	1,660 - 9,680	0.77
Ayat, Central Ural Mtn. region, U.S.S.R.	10:461	3,510 - 9,780	0.31
Bog Remmeski, Estonia	13:79	2,560 - 10,770	1.03
Kalina, Estonia	12:239	1,415 - 9,130	0.39
Niederwil, Switzerland	14:43	4,960 - 12,780	0.45?
Padul IV, Spain	14:30	4,980 - 46,440, and >54,000	1.55
Disterhaft Farm, Wisconsin	13:479	2,850 - 15,560	0.65
Pretty Lake, Indiana	11:144	920 - 13,375	0.67
Colo Bog, Iowa	10:255	3,100 - 13,775	0.64
McCulloch Bog, Iowa	10:258	3,170 - 14,500	0.46
Woden Bog, Iowa	10:258	2,830 - 11,570	1.22
Brown's Lake, Ohio	11:145	565 - 10,915	0.68
Muscotah, Kansas	12:321	5,100 - 23,040	3.33*
SEDIMENT			
Kaisungor B, Kenya	12:447	765 - 27,750	2.78
Lake Elmenteita, Kenya	14:120	8,740 - 29,320	0.51
Lake Victoria, Uganda	11:551	860 - 9,550	0.28
Lake Huleh, Israel	11:591	2,480 - 32,900	0.80
Lake Jih Tan, Taiwan	11:597	4,200-35,500 and >47,000	1.15
Lake Yueh Tan, Taiwan	11:551	1,280 - 9,670	0.85
Lake Keilambete, Australia	12:568	610 - 14,300	1.27
S.W. Australia coast	9:280	5,900 - 10,000 and >25,000	0 - 1.90 [0.95]
Blea Tarn, England	15:557	4,476 - 9,872	0.38
Nant Ffrancon, Wales	15:157	4,256 - 10,080	0.60
Lake Vuolep Njakajaure, Sweden (deep)	11:443	2,410 - 8,980	0.65*
Ranviken Bay, Sweden	11:431; 12:536	750 - 12,670	1.06
Striern, Sweden	12:541	740 - 12,090	1.03
Könkäänlampi, Finland	16:254	1,660 - 9,680	1.18

TABLE 1 (continued)

Lake Pappilanlampi, Finland	11:068	9,200 - 20,800	2.06 - 2.26 [2.16]
Dolni Véstonice, Czechoslovakia(loess)	9:100	15,350 - 49,900 and >52,000	0.86?
Plöner See, N.W. Germany	13:327	1,140 - 10,810	2.55
Segeberger See, N.W. Germany	12:528	1,890 - 12,690	0.52
Selent Lake #I, N.W. Germany	15:272	380 - 10,170	1.74
Selent Lake #IV	15:274	920 - 17,390	2.16
Selent Lake #VI	15:276	780 - 30,930	3.90
Boniger See #I, Switzerland	12:367	6,030 - 10,430	1.20
Boniger See #2	12:367	2,700 - 8,370	0.85
Charcot Seamount, N.E. Atlantic	16:091	3,800 - 26,500 and >35,000	0.36
Golf du Lion, France(shell)	15:324,328	6,900 - 31,500	1.14
Longetray, France (rockshelter charcoal)	15:524	4,640 - 12,720	0.59?
Venice composite, Italy	Nature 244:339	5,000 - 46,000	2.03
Antifreeze Pond, Alaska	13:302	5,690 - 29,700 and >36,000	1.05
Lake Hill, Alaska	11:563	2,620 - 17,800	1.25 - 1.76 [1.50]
Lofty Lake, Alberta	13:289	3,460 - 11,400	0.58
Lake Quassapaug, Connecticut	11:567	1,020 - 12,330	0 - 0.76 [0.38]
Rogers Lake, Connecticut	11:550	630 - 10,510	0.80
Berry Pond, Massachusetts	15:360	995 - 12,680	1.30
Bog D, Minnesota	11:576	2,720 - 11,000	0.98
Rutz Lake, Minnesota	11:573	1,100 - 12,000	0.40
Kalaloch, Washington	11:579	16,700 - 42,700 and >47,000	1.34
Rockyhock Bay, N. Carolina	15:360	6,655 - 25,020	2.12
Singletary Lake, N. Carolina	10:263	5,750 - 35,800 and >40,000	1.11
Blake Plain C-19, W. Atlantic	15:393	4,130 - 15,995	1.53
Campeche Bank, Yucatan	9:314 10:347	16,340 - 40,7008 936 - 15,000 and >41,000	1.983.35

Data for the features that have been included in this study are presented in Table 1. This listing contains all significant localities that have well-established profile trends to or beyond 9000 B.P. as given in *Radiocarbon*, vols. 8-16 (1966-1974; vol.16, #3 is not included), and selected features from volume 5. Also included is a summary of data for the Venice coastal region that were published in *Nature*, vol 244 (1973). Since a subjective element is involved in curve plotting and determination of appropriate values for δ and γ , individuals who may wish to check this data should not expect to always agree precisely with the author's selection of shape

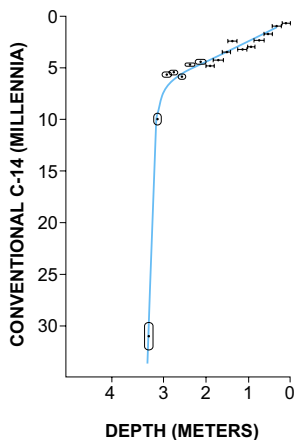


FIGURE 6. VARIANT C-TYPE PROFILE. Selent Lake VI (See Table 1).

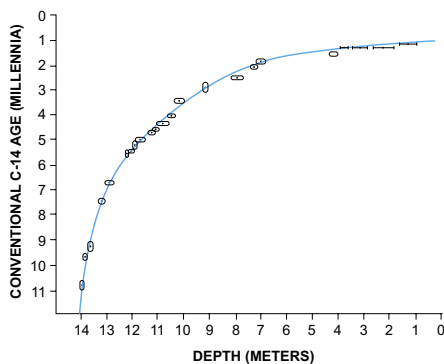


FIGURE 7. VARIANT C-TYPE PROFILE. Plöner See (See Table 1).

factor. Cases for which significant uncertainties exist are indicated in Table 1. An effort has been made to bias shape factor determinations toward zero (straight-line type profile) while being open-minded toward non-zero possibilities so that any conclusion reached will be trustworthy.

ANALYSIS OF COMPOSITE PROFILE CHARACTERISTICS

The profile shape factors from Table 1 are plotted in Figure 8. In this plot, shape factors have been grouped within ranges 0.25 shape factor units in width. Thus all shape factors between +1.00 and +1.24 are plotted in the first column to the right of +1. Those between +1.25 and +1.49 are plotted in the next column. All profiles for which $-0.24 < S < +0.24$ have been classified as A-type; and all profiles visually judged to be satisfactorily described by a straight line have been assigned a shape factor of zero and arbitrarily plotted between -0.25 and +0.25. According to this convention any profile for which $-0.22 < (\delta/\gamma) < +0.28$ is considered to be A-type, i.e., departure of the extreme age point from a linear relationship is within approximately one-fourth the C-14 age range of the curved portion of the profile.

Table 1 contains 98 features. Of these 22 or 22.4% have A-type profiles, 13 or 13.3% have B-type profiles, and 63 or 64.3% are C-type. The average shape factor for these profiles is 0.60 (within the third column between 0 and +1 of Figure 8), which corresponds to an average d/g

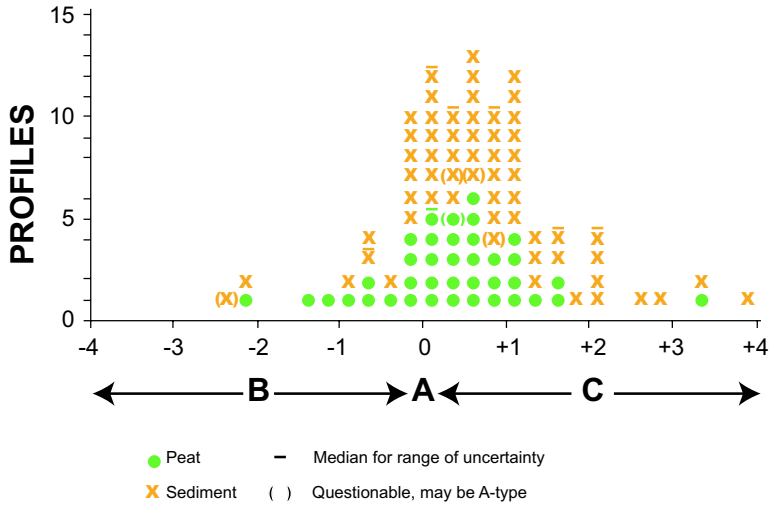


FIGURE 8. PROFILE SHAPE FACTOR SUMMARY. Number of profile shape factors failing within a given integral range 0.25 shape factor units in width. Profiles visually judged to be best represented by a straight line (A-type) are arbitrarily plotted between -0.25 and +0.25.

value of 0.82. Since the features for which this average has been computed do not all have an identical C-14 age range nor inflection at the same C-14 age, a quantitative interpretation of this average is uncertain. The value 0.82 is large enough to positively rule out compaction as the primary cause for the predominance of C-type profiles.

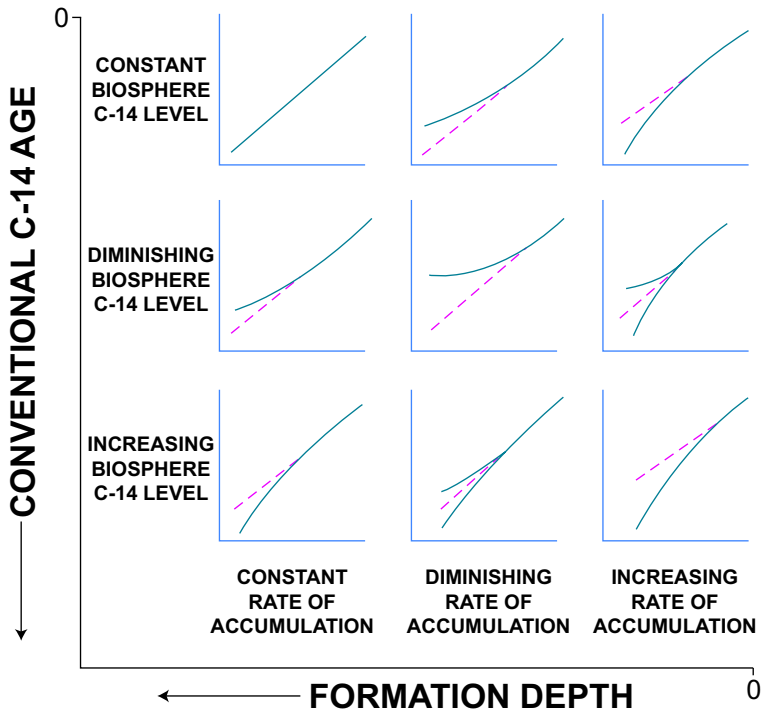
It seems to be clearly established that the predominant tendency is for ancient peat bogs and sediments to have a C-type profile. The various possibilities for profile development are given an idealized representation in Figure 9. A constant relative C-14 level in the biosphere and a uniform rate of accumulation will produce a perfect A-type profile, as shown in the upper left corner of Figure 9. Opposing changes in the C-14 activity level and the rate of accumulation can also fortuitously combine to produce an A-type profile, as indicated at the right of the second row and in the center of the third row of Figure 9. A C-type profile is seen to be the result of an increasing rate of formation, an increasing level of C-14 activity in the environment, or a combination of increase in both factors.

CONCLUSIONS

Explanation in terms of an increasing rate of formation accumulation for the 64% tendency toward C-type profiles found in this study requires

conditions that were relatively unfavorable, on the average, for peat bog growth and sediment accumulation (erosion) over the time covered by C-14 ages ranging between approximately 5000 B.P. and in the order of 30,000 B.P. The requisite conditions are a warm, dry climate or an arctic climate. Such conditions are not in accord with prevailing concepts concerning glaciation and ancient climate (Flint 1971); nor are they in accord with deductions concerning the probable consequences of a recent worldwide flood. These considerations, combined with recognition of the extremely steep early portions of those peat bog and sediment profiles that extend to the 30,000 and 40,000 B.P. regions, suggest explanation predominantly in terms of an increase in the relative C-14 level of the biosphere. This explanation also contributes to a rational basis for harmonizing C-14 ages with the chronological implications of the first eleven chapters of Genesis.

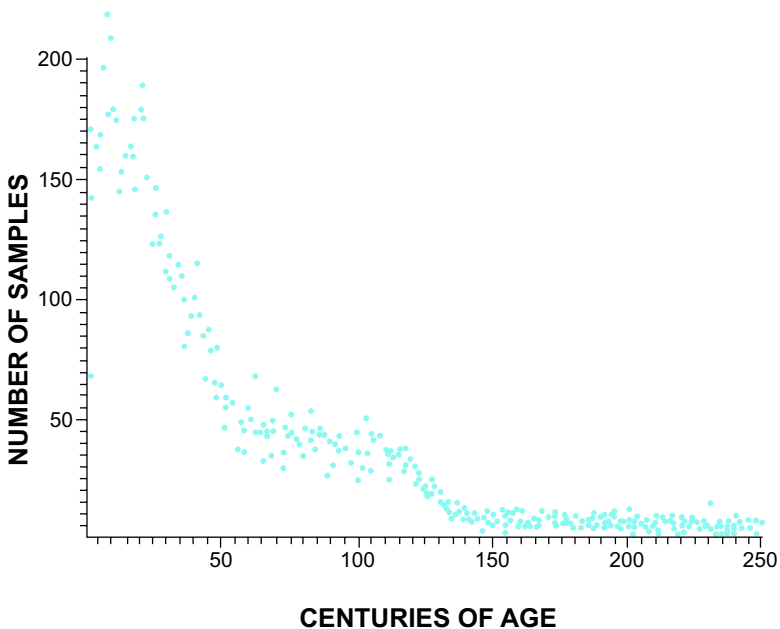
FIGURE 9. PROFILE INTERPRETATION GUIDE.



The existence of A- and B-type profiles for periods which are predominantly characterized by C-type may be accounted for as the consequence of local situations in which the initial rate of bog growth or sediment accumulation was so rapid as to counteract or overbalance, respectively, the effect of increasing C-14 activity on the feature profile. Such conditions may be expected during a period of cool pluvial climate, particularly when vegetation is being reestablished.

The suggestion that the specific C-14 activity in the biosphere was increasing as a general trend during prehistoric time is reinforced by Figure 10. In this figure over 10,000 radiocarbon age determinations that were reported between 1950 and 1965 are plotted versus centuries of C-14 age. Although it may be argued that the C-14 dating results available by the end of 1965 contain a representative sampling of the entire age range, it also should be recognized that accessibility and archaeological interests probably have favored a disproportionate collection of recent

FIGURE 10. FREQUENCY OF SAMPLES AS A FUNCTION OF C-14 AGE. Data from: Deevey ES, Flint RF, Rouse I, editors. 1967. Radiocarbon Measurements: Comprehensive Index, 1950-1965. New Haven, CT: Yale University Press. Plot courtesy Dr. H. C. Sorensen.



and intermediate dates. With due allowance for such possible bias, Figure 10 indicates plateaus in the availability of C-14 dates over the C-14 age ranges of 30,000-14,000 and 12,000-6,000.

These plateaus could indicate periods of rapid increase in the specific C-14 activity of the biosphere. During such periods the average specific C-14 activity of organisms at death would be constantly increasing, with production of a smaller number of specimens with a given initial activity level than would be the case under a constant level of C-14 activity. For such specimens a ± 50 year “window” in present measurement of residual activity would correspond with only a few years or possibly months during growth. Accordingly, the representation in Figure 10 could indicate rapid increase in the biosphere C-14 activity level during the period corresponding to 30,000-14,000 C-14 years, less rapid increase in this level over the period corresponding to 12,000-6,000 C-14 years, and approximate constancy of this level over the past 3,000 years (as confirmed by historical and dendrochronological calibration). Transitions would occur during the intervening periods.

A rapidly increasing C-14 activity level in the supporting environment also accounts for the anomalous C-14 ages associated with the Chekurovka mammoth — 26,000 for hair and 5,610 for overlying peat (*Radiocarbon* 8:320, 321); the Fairbanks Creek musk ox — 24,000 for scalp muscle tissue and 17,200 for hair (*Radiocarbon* 12:203); the Union Pacific mammoth — 11,300 for most recently formed ivory and 5,000 for wood fragments in the surrounding gravel (*Radiocarbon* 8:172, 173); and the Ferguson Farm mastodon — 8,900 for bone collagen and 6,200 for gyttja from within skull cavities (*Radiocarbon* 10:216).

The data covered in this report do not support the 10% decrease in biosphere C-14 activity level required by the currently accepted bristlecone pine master chronology between 5500 B.P. and 2500 B.P., unless it can be established that there has been a preponderant tendency for increased rates of sediment accumulation and bog growth over the past 5,000 years. This conclusion gains greater force on a detailed examination of the individual profiles listed in Table 1 (the g region of one-half the C-type profiles listed begins between approximately 5000 and 10,000 B.P., with one-fourth beginning below and one-fourth beginning above this range).

A general trend of increasing biosphere C-14 specific activity levels over the range of real time covered by C-14 ages between 40,000 and 5000 B.P. is strongly indicated, if not well established, by this study. Consequently C-14 ages in the prehistoric range should be expected to be progressively in excess of the real time involved.

Further refinement and expanded development on the suggestions contained in this report should prove fruitful. For example, it would be

desirable to determine the average profile trends for various geographical regions and for various portions of the C-14 age range.

LITERATURE CITED

- Flint RF. 1971. Glacial and quaternary geology. NY: John Wiley and Sons, Inc., specifically Ch 16.
- Libby WF. 1955. Radiocarbon dating. 2nd edition. Chicago: The University of Chicago Press.
- Olsson IU, editor. 1970. Radiocarbon variations and absolute chronology. NY: Wiley Interscience Division, John Wiley and Sons, Inc.
- Ralph EK, Michael HN, Han MC. 1973. Radiocarbon dates and reality. MASCA Newsletter 9(1). Applied Science Center for Archaeology, University Museum. Philadelphia: University of Pennsylvania.